Atmospheric Environment 44 (2010) 1400–1413

Contents lists available at ScienceDirect

Atmospheric Environment

journal homepage: www.elsevier.com/locate/atmosenv

Influence of ship emissions on air quality and input of contaminants in southern Alaska National Parks and Wilderness Areas during the 2006 tourist season

Nicole Mölders [a,*], Stacy E. Porter [a], Catherine F. Cahill [b], Georg A. Grell [c]

[a] University of Alaska Fairbanks, Geophysical Institute & Department of Atmospheric Sciences, 903 Koyukuk Dr., Fairbanks, AK 99775-7230, USA
[b] University of Alaska Fairbanks, Geophysical Institute & Department of Chemistry and Biochemistry, 903 Koyukuk Dr., Fairbanks, AK 99775-7230, USA
[c] NOAA/Earth System Research Laboratory, 325 Broadway, Boulder, CO 80305-3337, USA

ARTICLE INFO

Article history:
Received 21 July 2009
Received in revised form
27 January 2010
Accepted 1 February 2010

Keywords:
WRF/Chem
Ship emissions
Pollution
Bottom–up ship-emission inventory

ABSTRACT

The impact of ship emissions on air quality in Alaska National Parks and Wilderness Areas was investigated using the Weather Research and Forecasting model inline coupled with chemistry (WRF/Chem). The visibility and deposition of atmospheric contaminants was analyzed for the length of the 2006 tourist season. WRF/Chem reproduced the meteorological situation well. It seems to have captured the temporal behavior of aerosol concentrations when compared with the few data available. Air quality follows certain predetermined patterns associated with local meteorological conditions and ship emissions. Ship emissions have maximum impacts in Prince William Sound where topography and decaying lows trap pollutants. Along sea-lanes and adjacent coastal areas, NO_x, SO_2, O_3, PAN, HNO_3, and $PM_{2.5}$ increase up to 650 pptv, 325 pptv, 900 pptv, 18 pptv, 10 pptv, and 100 ng m^{-3}. Some of these increases are significant (95% confidence). Enhanced particulate matter concentrations from ship emissions reduce visibility up to 30% in Prince William Sound and 5–25% along sea-lanes.

1. Introduction

High concentrations of primary pollutants are emitted along sea-lanes. In Alaska, this situation is especially true for the Gulf of Alaska, where tankers, cargo ships, and ferries sail its sea-lanes. During Alaska's summer, additional fishing boots, charter vessels and tourist cruises cause a distinct peak of ship emissions. Ship cruises – about 1 million tourists experience Alaska on cruises – are a major factor in Alaska's economy. Tourism relies on the uniqueness of the coastal landscape. Showing off these attractions requires pristine water and good air quality to provide excellent visibility. The influx of pollutants from ship emissions and their transformations in the atmosphere may counteract the aesthetic attraction of popular tourist locations. Pollutants lower visibility, air and water quality, and are potentially hazardous for ecosystems and wildlife. Thus, the coastal waters of Alaska represent a tourism paradox where the attraction causes its own destruction.

The Regional Haze Rule aims at preserving visibility in National Parks and Wilderness Areas (Class-I-Areas). Four Class-I-Areas exist in Alaska. Two of them, the Tuxedni and the Simeonof Wilderness Area (Fig. 1), are remote, but close to sea-lanes.

The International Maritime Organization (IMO) regulates global ship emissions. The maximum allowed nitrogen oxides [NO_x(=NO + NO_2)] emission depends on the vessel's engine speed. The sulfur content of the fuel burned determines the amount of sulfur dioxide (SO_2) emitted. The fuel of oceangoing vessels contains 2.7% sulfur on average, but up to 4.5% maximally.

In Alaska, existing regulations primarily address aesthetic aspects related to tourism attractions. Ships within three miles of the Alaska coast may not degrade visibility within the exhaust effluent by 20% within an hour. Due to these modest regulations, ships can release substantial amounts of pollutants into the relatively clean marine atmospheric boundary layer (ABL).

Some primary pollutants react chemically with trace species naturally available in the atmosphere, while others are modified photo-chemically during the long daylight hours of Alaska's summer. The resulting secondary pollutants may be transported into coastal regions under various weather situations. Over land, pollutants react with volatile organic compounds (VOCs) emitted by vegetation. The concurrent processes of transport and transformation of trace species may lead to high pollutant concentrations, even in remote areas adjacent to oceans like southern Alaska's National Parks and Wilderness Areas.

Various processes (transport, turbulence, evapotranspiration, sorption, desorption, biogenic activity, emission, settling, chemical reactions) are involved in the dry deposition process. Thus, dry deposition not only depends on the physical and chemical states of

* Corresponding author. Tel.: +1 9074747910; fax: +1 9074747290.
E-mail address: molders@gi.alaska.edu (N. Mölders).

1352-2310/$ – see front matter © 2010 Elsevier Ltd. All rights reserved.
doi:10.1016/j.atmosenv.2010.02.003

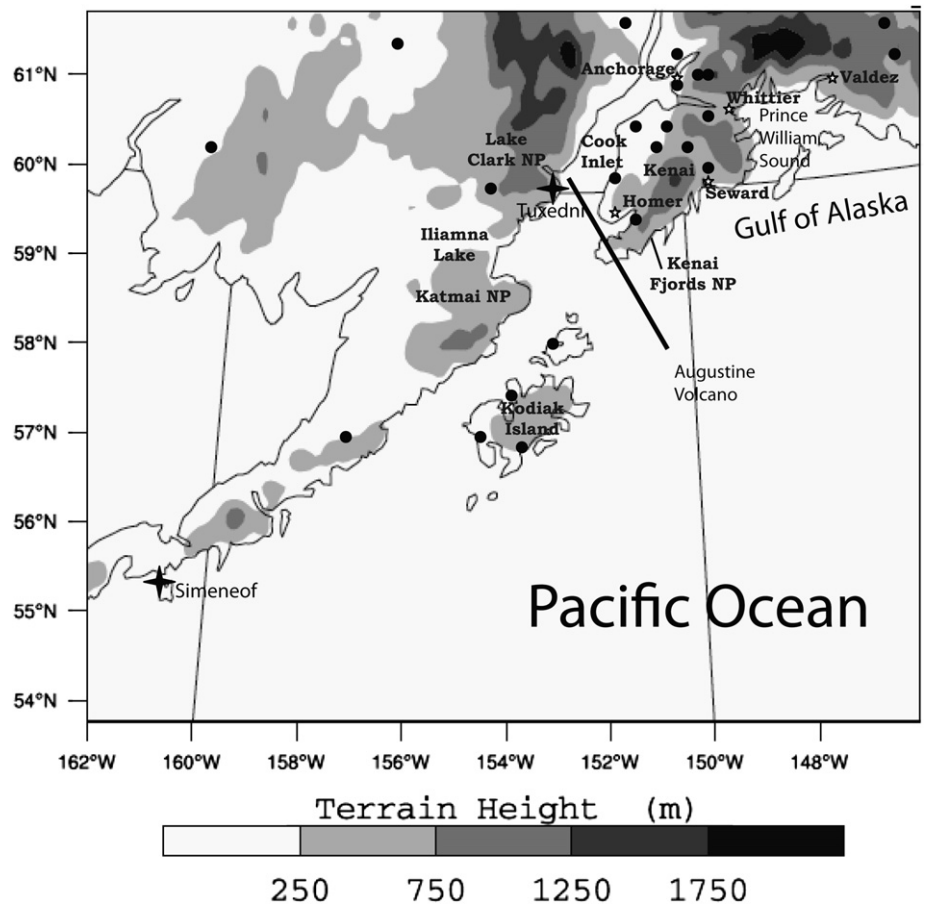

Fig. 1. Terrain height, location of National Parks (NP) and wilderness areas, meteorological (dots) and aerosol measurement sites (stars).

the atmosphere, but also on the surface on which the trace gases and particles deposit (Wesley, 1989; Kramm et al., 1995). Wet deposition is related to the scavenging of gases and particles in and below the cloud and to precipitation (Walcek and Taylor, 1986). Both wet and dry deposition represent burden on the ecosystems and natural water systems.

Various scientists (e.g. Endresen et al., 2003; Lelieveld et al., 2004; Eyring et al., 2005) examined the impact of ship emissions on the global-scale with focus on regions with midlatitude-humid or Mediterranean climate. Simulations with a global chemistry transport model indicate that ship emissions increase NO_x and ozone (O_3) by a factor of two and hydroxyl radical (OH) by 20% over oceans, and increase NO_x and OH by a factor of two and five, respectively within sea-lanes (Lawrence and Crutzen, 1999). About 30% of Northern Hemispheric SO_2 stems from ship emissions; sulfur from ship emissions contributes to atmospheric SO_2 in a comparable magnitude as dimethyl-sulfide emissions from algae; in the Northern Hemisphere, Arctic and eastern Pacific and coastal regions, ship emissions contribute 10–30%, 30–50% and 5–20%, respectively to the sulfate concentrations (Capaldo et al., 1999). Ship emissions initiate 5–20% of the O_3 concentrations and 50–55% of the sulfur deposited in Europe (Derwent et al., 2005).

Due to the photo-chemical and climatic differences, one cannot assess the impact of ship emissions in southern Alaska from midlatitude studies. In midlatitudes, the chemical processes (daytime chemistry) differ from those at night (nighttime chemistry). During Alaska summer, the sun hardly goes below the horizon and provides energy for photo-chemical processes for nearly 24 h.

The goal of our study was to assess the impact of ship emissions on air quality, and the atmospheric input of highly reactive oxidants and acidic contaminants into southern Alaska's National Parks and Wilderness Areas during a tourist season. We performed illustrative simulations with WRF/Chem (Grell et al., 2005; Peckham et al., 2009) with and without consideration of ship emissions for the length of the 2006 tourist season.

2. Experimental design

2.1. Model description

WRF/Chem is based on the **W**eather **R**esearch and **F**orecasting (WRF; Skamarock et al., 2008) model inline coupled with a chemistry package. It predicts the weather and describes trace-gas cycles from emission, through a variety of chemical reactions and transport, to wet or dry deposition.

We chose the following physical packages that typically capture Alaska weather situations well (Mölders, 2008; Mölders and Kramm, 2010): The 6-class microphysics (Hong and Lim, 2006), a version of the Grell and Dévényi (2002) cumulus-ensemble approach, Dudhia's (1989) shortwave and Mlawer et al.'s (1997) long-wave radiation schemes, Janjić's (2002) schemes for the viscous sub-layer and ABL, and a modified version of Smirnova et al.'s (2000) land-surface model.

We chose the standard well-tested chemical setup (McKeen et al., 2007) which includes the following packages. The RADM2 (Regional Acid Deposition Model, version 2) gas-phase chemical mechanism (Stockwell et al., 1990) considers 14 stable, four reactive

intermediate, and three abundant stable inorganic species (oxygen, nitrogen, water). It represents atmospheric organic chemistry with 26 stable species and 16 peroxy radicals. Photolysis frequencies for the 21 photo-chemical reactions considered were calculated following Madronich (1987). Dry deposition of trace gases follows Wesley (1989). The MADE/SORGAM (Modal Aerosol Dynamics Model for Europe/Secondary Organic Aerosol Model; Binkowski and Shankar, 1995; Ackermann et al., 1998; Schell et al., 2001) considers the physics and chemistry of inorganic aerosols, secondary organic aerosols including wet and dry removal. Biogenic emissions by vegetation and nitrogen emissions by soil were calculated considering temperature and photosynthetic active radiation (Guenther et al., 1994; Simpson et al., 1995).

2.2. Ship-emission inventory

To consider ship emissions, a sea-lane-related emissions inventory was developed following Corbett and Köhler (2003). This bottom–up approach is based on ship time tables, port times, and routes of tankers, container ships, roll-on/roll-off cargo ships, cruise ships, ferries and fishing boats. It considers data on the typical fuel usage of these vessels and the typical split among the species released in combustion processes (Fig. 2).

The following assumptions were made (Porter, 2009): Most cruise ships use medium-speed, four-stroke diesel engines, while tankers and cargo ships use slow-speed, two-stroke diesel engines (Corbett et al., 2007). All main engines use residual oil. About 71% of the vessels use residual oil for the auxiliary engines as well. Tanker auxiliary engines use distillate fuel.

Independent of their size, the average engine power of cruise ships, tankers, container and cargo ships were assumed as 39 563, 9409, 30 885 and 10 696 kW, respectively (Corbett et al., 2007). Average auxiliary power was assumed proportionally to the main power as 10 682, 3293, 8339 and 4172 kW using a ratio of 0.27, 0.35, 0.27 and 0.39 for cruise ships, tankers, container, and cargo ships, respectively.

The inventory considers cruising, maneuvering and berthing. These operation modes affect the emission factors of carbon monoxide (CO), VOC and particulate matter (PM) (Cooper and Gustafsson, 2004). Cruising dominates. In accord with ENTEC UK Limited (2002), maneuvering lasts 1 h before and after port call. Berthing occurs in port to maintain power. Except for tankers, ships only use the auxiliary engines during berthing. Cruising ships were assumed to have a main engine load of 80% and auxiliary engine load of 30%. Berthing was assigned a 60% load of the auxiliary engines except for tankers that were assigned a 20% and 60% load to the main and auxiliary engines, respectively. Maneuvering uses 20% of the main and 50% of the auxiliary engine load.

Emission factors are available from ENTEC UK Limited (2002) for NO_x, SO_2, VOCs and PM, from Cooper and Gustafsson (2004), Corbett et al. (2007) for CO, and Cooper and Gustafsson (2004) for ammonia (NH_3). The PM emission factor was used for both $PM_{2.5}$ and PM_{10}. Following ENTEC UK Limited (2002), we assumed 90% of the PM emission is $PM_{2.5}$. VOCs were split among ethane, butane, formaldehyde, pentane, hexane, ethylene, propylene, acetylene, benzene, toluene, xylene, tri-methylbenzene, and other aromatics following Eyring et al. (2005). $PM_{2.5}$ was split among sulfate, organic and elemental carbon, and unspecified $PM_{2.5}$ following Petzold et al. (2004).

Hourly emissions as a function of latitude and longitude were calculated based on the emission factors, average power, and load factors of the main and auxiliary engines. Fig. 3 illustrates the emissions of SO_2 obtained for the emission inventory developed for this study.

2.3. Simulations

The model domain encompasses the atmosphere over south Alaska with 27 stretched vertical layers and 151 × 128 grid-points in the horizontal using a grid-increment of 7 km (Fig. 1).

The initial and boundary conditions for the meteorological, snow and soil variables stemmed from the 1.0° × 1.0° and 6 h-resolution

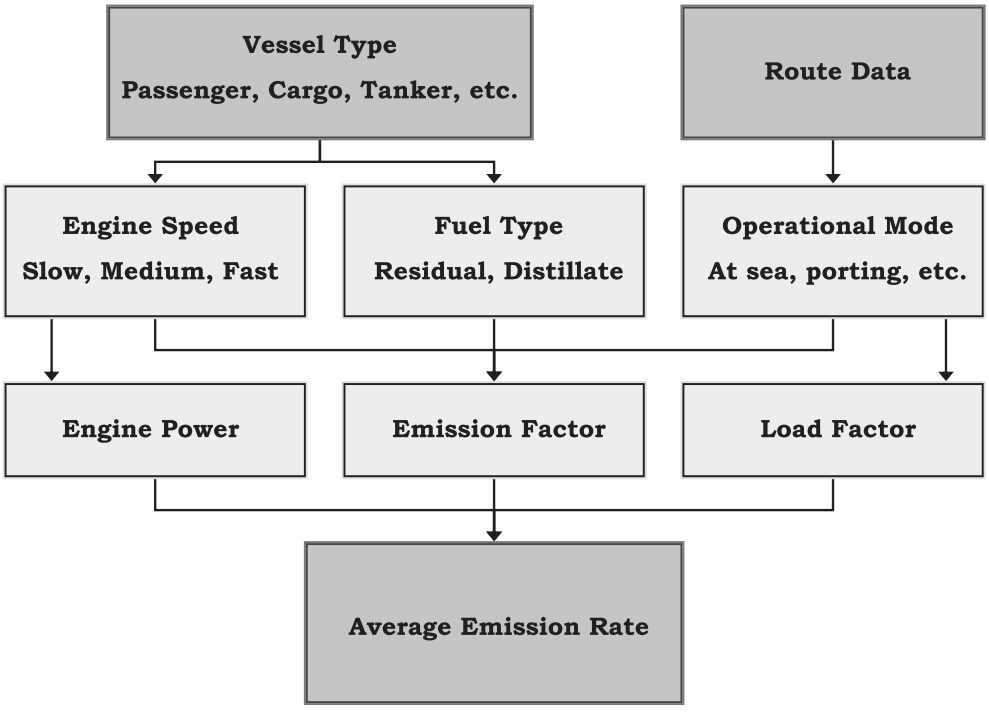

Fig. 2. Schematic view of the emission inventory.

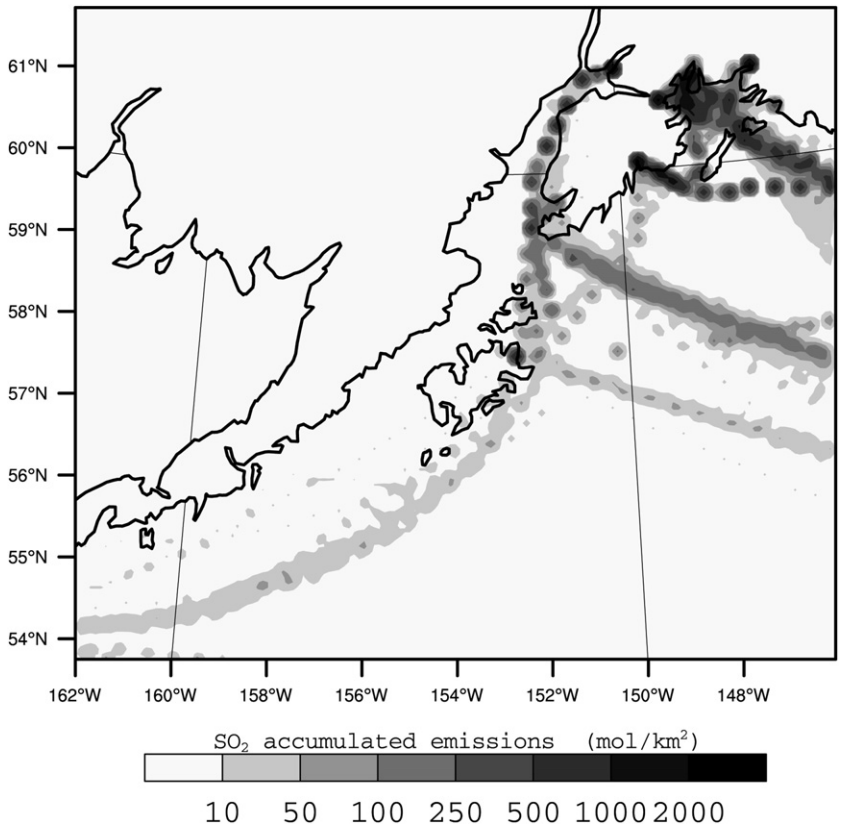

Fig. 3. Horizontal distribution of accumulated SO_2 emissions from ships for the tourist season 2006. Distributions of other species look similar.

National Centers for Environmental Prediction global final analyses (FNL) data. WRF/Chem was initialized with idealized vertical profiles of Alaska background concentrations. It was run from May 15 to 20, 2006 to spin up the chemical compound fields. The chemical distribution, obtained for May 20, 2006 served as the initial distribution for the first day of our study (May 20, 2006). All later simulations used the chemical distributions obtained at the end of the previous simulation as chemical initial conditions. We ran 5-day simulations without (REF) and with (SEM) inclusion of ship emissions until August 20, 2006. Note that investigations with daily restarts showed that when using FNL-data as initial/boundary conditions, 120 h-simulations only marginally differ in quality from 24 h-simulations (Mölders, 2008).

2.4. Analysis

Hourly observations of temperature, dewpoint temperature, relative humidity, precipitation, sea-level pressure, wind-speed, and downward shortwave radiation exist for 24 sites (Fig. 1); due to the remote location, no chemical measurements are available. Aerosol measurements are sparse in Alaska. The Interagency Monitoring of Protected Visual Environments program collects $PM_{2.5}$ and PM_{10} once every three days and determines their mass and composition (organic carbon, elemental carbon, trace elemental species, key ions, etc.). Only two sites of this network exist within the area of interest (Fig. 1). Nevertheless, for completeness we included this limited aerosol data in our evaluation.

Student's *t*-tests served to test the hypotheses that simulated and observed data do not differ and ship emissions have no impact on air quality, visibility, and deposition. We used the 95% confidence level. The response of air quality, visibility and deposition fluxes to ship emissions was examined for the length of the 2006 tourist season by comparison of the results from REF and SEM.

3. Results

3.1. Evaluation

Various evaluations of the meteorological part of WRF/Chem have been performed for Polar Regions (e.g. Hines and Bromwich, 2008; Mölders, 2008). WRF/Chem showed itself able to simulate the poor air quality conditions for a variety of cases in midlatitudes (e.g. Grell et al., 2005; Eder et al., 2005; McKeen et al., 2007; Bao et al., 2008).

For the 2006 tourist season, errors are of similar magnitude to those found for other WRF-simulations in Polar Regions (e.g. Hines and Bromwich, 2008; Mölders, 2008) and other modern numerical weather prediction models elsewhere (e.g. Zhong et al., 2005; Papalexiou and Moussiopoulos, 2006). WRF/Chem captures the temporal evolution of all quantities except for some delays at certain sites during frontal passages (Fig. 4). WRF/Chem overestimates sea-level pressure, wind-speed, precipitation, dewpoint temperature and relative humidity by 3 hPa, 1.8 m s^{-1}, 0.04 mm, 1.8 K and 10%, respectively, when averaged over the tourist season. WRF/Chem underestimates (overestimates) the maximum (minimum) temperature by 3.7 K (0.8 K) on average. It slightly underestimates temperature (−1.6 K) and downward shortwave radiation (−11 W m^{-2}). Shortwave-radiation predictions are better on days with broken rather than total cloudiness (Fig. 4). The underestimation of temperature and shortwave radiation may be due to errors in predicted cloudiness.

WRF/Chem overestimates wind-speed more under low than high-pressure regimes (Fig. 4) which may affect PM-production

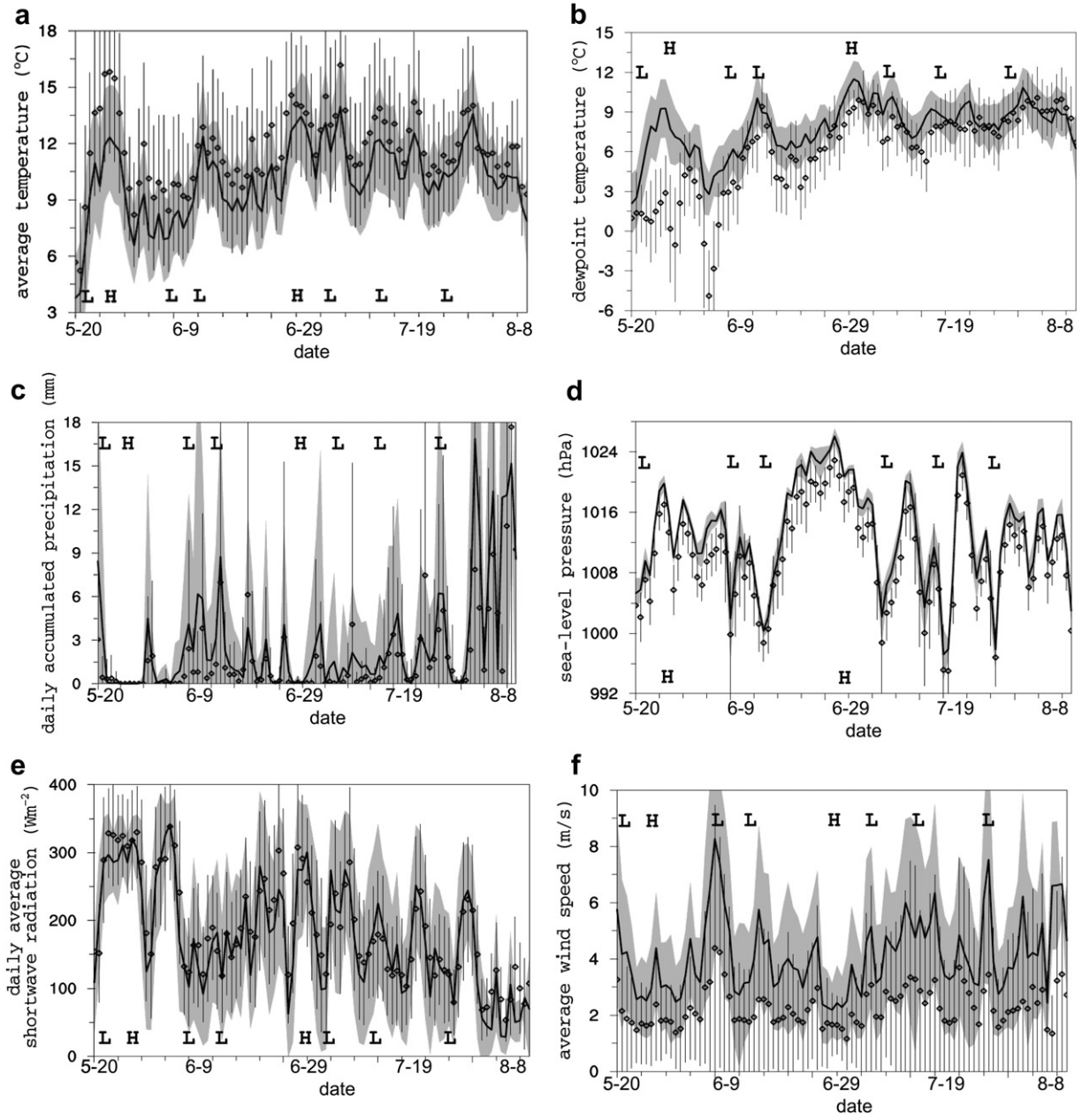

Fig. 4. Time series of daily averages of observed (diamonds) and predicted (solid line) (a) temperature, (b) dewpoint temperature, (c) precipitation, (d) pressure, (e) downward shortwave radiation, and (f) wind-speed, averaged overall 24 sites. The gray area and vertical bars represent standard deviations with respect to the sites for the simulation and observations. L and H indicate low or high-pressure.

from sea-spray. WRF/Chem better predicts relative humidity and dewpoint temperatures under moist over dry conditions. WRF/Chem dampens the strength of drops in dewpoint temperatures during high-pressure systems that advect very dry air from Interior Alaska (e.g. June 4–9, Fig. 4).

Errors for individual sites or at specific times may be slightly larger or lower than these averages over all sites or the entire period. At sites in valleys, channeling effects may lead to notable discrepancies between simulated and observed wind-direction. Except for these effects and frontal offsets/delays, WRF/Chem captures the main wind-direction well on average.

Underestimation of temperature may affect concentrations of species that are subject to thermal depletion. The slight overestimation of relative humidity and precipitation may affect simulated cloudiness, precipitation, photolysis-rates, and wet deposition. The underestimation of shortwave radiation may affect temperature, thermal decomposition and photolysis-rates.

The standard deviation of errors (SDE) is of similar magnitude to the absolute bias for temperature, dewpoint temperature, and relative humidity. Random errors from initial and boundary conditions govern errors in wind-speed and shortwave radiation. Errors from initial and boundary conditions are similar to those obtained when using other reanalysis data.

Accuracy of predicted precipitation is 93% and 71% for daily and hourly values. The daily and hourly categorical bias-scores of 1.3 and 1.1 indicate that WRF/Chem tends to predict falsely more precipitation than it misses in an actual event. The probability of detection is 99% and 89% for daily and hourly precipitation. Thread-scores are 0.92 and 0.61 for daily and hourly precipitation. The daily and hourly Heidke-skill scores of 0.429 and 0.396 are

slightly better than those of Mölders' (2008) WRF-June simulations over Interior Alaska.

The performance skills may be biased slightly due to misrepresentation of the landscape. PaiMazumder and Mölders (2009) reported that site locations affect notably the regional averages determined. Thus, the somewhat clustered distribution of sites – eight of 24 sites are on Kenai Peninsula (Fig. 1) – may give preference to phenomena related to certain terrain features, while totally omitting others.

Despite an overall evaluation by only two sites is impossible, we included a comparison of the results with the aerosol measurements for completeness. WRF/Chem broadly captures the temporal evolution of the aerosol concentrations most of the time (Fig. 5). It consistently underestimates $PM_{2.5}$ and PM_{10} at both sites by on average -2.3 μg m^{-3} and -5.8 μg m^{-3}, respectively. Root mean square errors and SDE are 2.7 μg m^{-3} and 1.5 μg m^{-3} for $PM_{2.5}$ and 8.8 μg m^{-3} and 6.7 μg m^{-3} for PM_{10}. The similar magnitude of bias and SDE indicates that both systematic and random errors contribute to the overall error.

Investigation shows that errors associated with initial and boundary conditions include advection of PM from wildfires and SO_2 emissions from volcanoes. The huge discrepancies between May 20 and June 9 coincided with wildfires in Interior Alaska and a wildfire close to Simeonof. Augustine Volcano (located in the Cook Inlet 270 km SW of Anchorage; Fig. 1) that erupted in January 2006, was still venting unknown amounts of SO_2, and other gases. In nature, these trace gases may have produced PM through gas-to-particle conversion. Neglecting the emissions from Anchorage may contribute to the systematic underestimation.

In some cases, spatial and/or temporal offsets in the positioning of low-pressure systems coincide with huge discrepancies in simulated and observed particle concentrations (e.g. July 9–14; Fig. 5). Simulated cloud-systems running ahead or being delayed yield notable differences between simulated and observed PM concentrations. Herein two processes contribute error: PM transport is predicted incorrectly in space and/or time and incorrect wind conditions lead to over/underestimation of PM formation from sea-spray.

All the aforementioned discrepancies apply similarly to REF and SEM. Thus, discrepancies between simulated and observed quantities should negligibly affect the overall results and conclusions on the impact of ship emissions on air quality and deposition of contaminants.

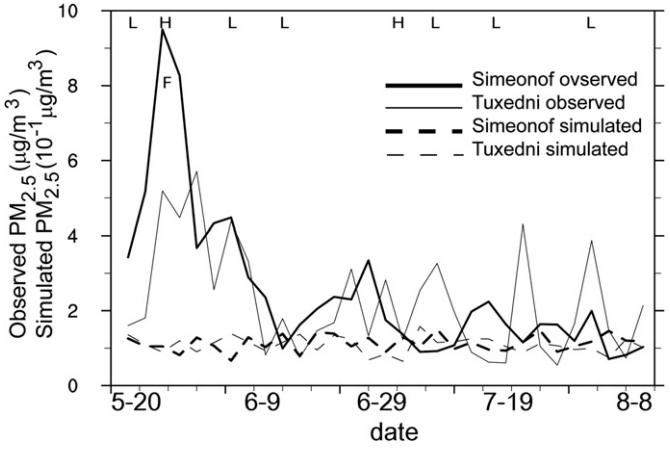

Fig. 5. Temporal evolution of daily average observed and simulated $PM_{2.5}$ concentrations. Observations exist every three days. PM_{10} shows similar behavior. F, L and H indicate wildfires, low and high-pressure.

3.2. General features

On domain average, the temporal evolution of primary concentrations and their deposition fluxes is similar for SEM and REF with SEM having higher values (Figs. 6–11). However, ship emissions locally cause notable and even significant differences.

In the Gulf of Alaska, low-pressure systems dominate the weather. They lead to onshore winds transporting pollutants from ship emissions onshore where the coastline is exposed to the east. Low-pressure systems tend to stagnate in and eventually dissipate in Prince William Sound due to the topography that acts as a barrier (Fig. 1). The resulting low wind-speeds from varying directions and the heavy ship traffic permit pollutants to accumulate in the atmosphere over the sound. Production of secondary pollutants is enhanced, as compared to better-ventilated areas, and dry and wet deposition increase in the sound.

Ship traffic to and from Anchorage mainly affects Lake Clark and Katmai National Parks. Since close to these parks no ports exist that would contribute notable amounts of PM through berthing and maneuvering, deposition of PM remains marginal.

Winds tend to converge and channel between the Kenai Peninsula and Kodiak Island. If a low-pressure system is located so that it has easterly winds, strong onshore winds form. This wind feature causes pollutants from ship emissions to travel further inland toward Iliamna Lake, a tourist/recreation attraction between Lake Clark and Katmai National Parks.

The ship emissions along the sea-lanes between Seward, Homer, and Anchorage strongly affect the Kenai Peninsula and Kenai Fjords National Park. Air quality decreases along the coast of the peninsula, and for some species, significantly.

Ozone concentrations are low over the tourist season and not as obviously related to topography as the primary and other secondary pollutants.

3.3. Nitrogen-oxides

Nitrogen-oxides concentrations are slightly higher over land than the ocean (Fig. 6) because of the increased nitric acid (HNO_3) formation from NO_2 and OH occurring over water. Generally, NO_x concentrations and deposition fluxes are reduced (enhanced) slightly during low-pressure (high-pressure) situations. The reduction of NO_x during low-pressure events results from HNO_3 formation and subsequent scavenging (Fig. 7). Thermal decomposition of peroxyacetyl nitrate (PAN) increases NO_x concentrations (e.g. around July 4, Figs. 6 and 8).

Due to its relatively short lifetime (<1 d), NO_x is not transported far away from its sources. NO_x significantly increases close to the sea-lanes especially in Prince William Sound (up to 650 pptv on average over the tourist season) and the Cook Inlet (Fig. 6). In Prince William Sound, about 90% and in coastal regions, about 50% of the NO_x deposition stem from ship emissions. This increased deposition may affect forested and freshwater ecosystems with low alkalinity close to sea-lanes and negatively affect the beauty of the landscape and fishing.

3.4. Sulfur-dioxide

The meteorological situations broadly govern the SO_2 concentrations (Fig. 9). For instance, SO_2 drops drastically during the precipitation associated with the low-pressure system around June 9. However, low-pressure systems can also accumulate SO_2 in the area despite increased deposition (e.g. around July 19).

Sulfur-dioxide concentrations show an overall decreasing trend throughout the tourist season (Fig. 9), while the deposition flux increases slightly. The increase of precipitation as summer

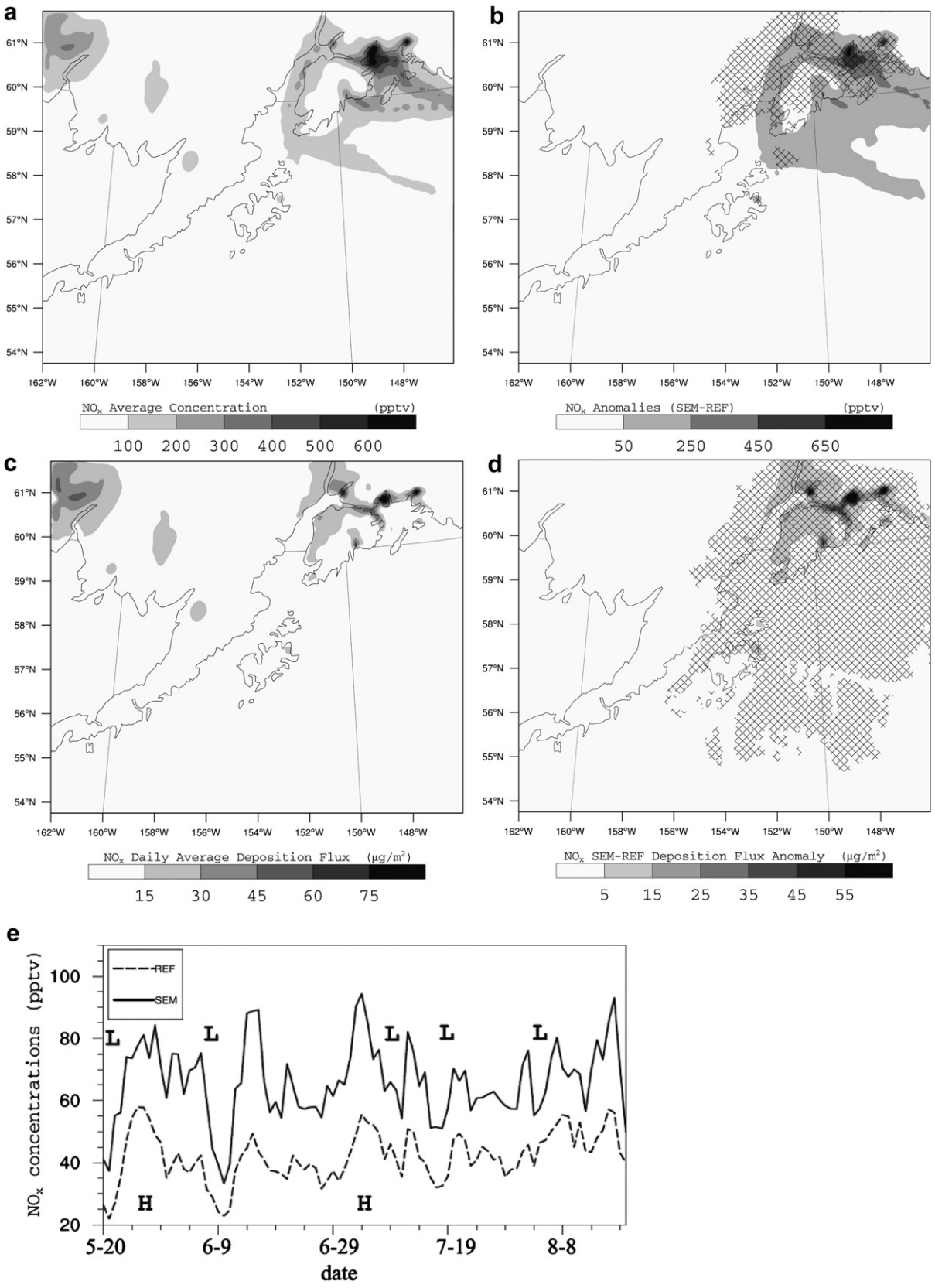

Fig. 6. NO_x: Horizontal distribution of seasonal-average concentrations (a) in SEM, (b) differences SEM−REF, (c) deposition flux, (d) deposition-flux differences, and (e) temporal evolution domain-average concentrations. L and H indicate low and high-pressure. Significant changes are hashed.

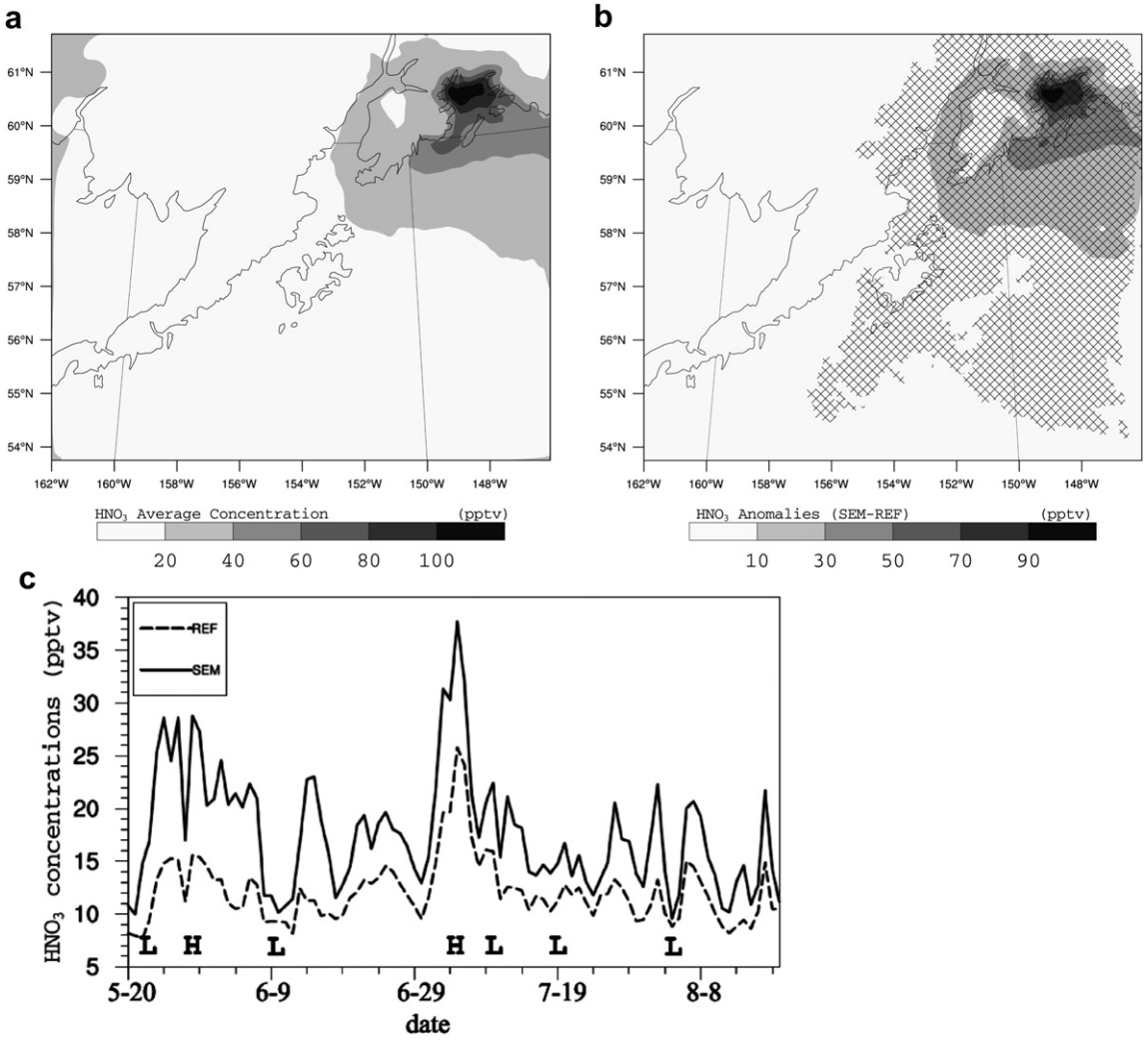

Fig. 7. HNO_3: Horizontal distribution of seasonal-average concentrations (a) in SEM, (b) differences SEM−REF, and (c) temporal evolution of domain-average concentrations. L and H indicate low and high-pressure. Significant changes are hashed.

progresses (Fig. 4) that is typical for the region (Shulski and Wendler, 2007), causes this behavior.

Ship emissions significantly (up to 325 pptv) increase the seasonal-average SO_2 concentrations along the sea-lanes and adjacent coastal areas (Fig. 9). Again, ship emissions contaminate Prince William Sound the most. Ship emissions contribute significantly to the SO_2 deposition in the Gulf of Alaska reaching 80–90% in Prince William Sound. This deposition may lower the pH-value of the uppermost water layers with adverse impacts for marine life.

3.5. Particulate matter

PM concentrations and deposition strongly depend on meteorological conditions (Fig. 10). As low-pressure systems approach, PM concentrations increase over the ocean due to churn up of sea-salt. As soon as precipitation begins, PM concentrations drastically drop due to wet removal (e.g. around June 9). Due to its coarse size and relatively high settling velocity, PM_{10} does not accumulate even during stable long-lasting high-pressure regimes, while $PM_{2.5}$ often does.

In spite of ship emissions, 24 h-average $PM_{2.5}$ concentrations remain below the National Ambient Air Quality standard (NAAQS) of 35 $\mu g\ m^{-3}$ everywhere (Fig. 10). Generally, the highest concentrations occur around port cities due to incomplete combustion during porting. Ship emissions significantly increase $PM_{2.5}$ concentrations up to 100 ng m^{-3} in the Gulf of Alaska. Areas along the sea-lanes are affected most. PM_{10} shows similar behavior except that significant impacts only occur around Anchorage and Valdez. Since only 10% of the PM emitted by ships is PM_{10}, and PM_{10} is larger, a smaller area experiences more significant concentration increases (locally $>$100 ng m^{-3}) than for $PM_{2.5}$. Ship emissions contribute about 30–40% and 10% to the total $PM_{2.5}$ and PM_{10} concentrations over the tourist season.

As concentrations of PM increase, scattering and absorption of light increase and reduce visibility. The $PM_{2.5}$ concentrations in SEM and REF are smaller than midlatitude background conditions. Therefore, in REF, visibility often exceeds 300 km. The enhanced PM concentrations due to ship emissions reduce visibility up to 30% in Prince William Sound and 5–25% along sea-lanes (Fig. 12). The ship emissions do not affect visibility in the Class-I-Areas.

Valdez and Anchorage experience enhanced $PM_{2.5}$ and PM_{10} deposition from incomplete combustion during berthing. Around Valdez, ship emissions contribute about 60% and more than 20% of the total $PM_{2.5}$ and PM_{10} deposition, respectively (Fig. 10). On average, ship emissions locally increase $PM_{2.5}$ and PM_{10} deposition by 50 to more than 90% in Prince William Sound and Anchorage.

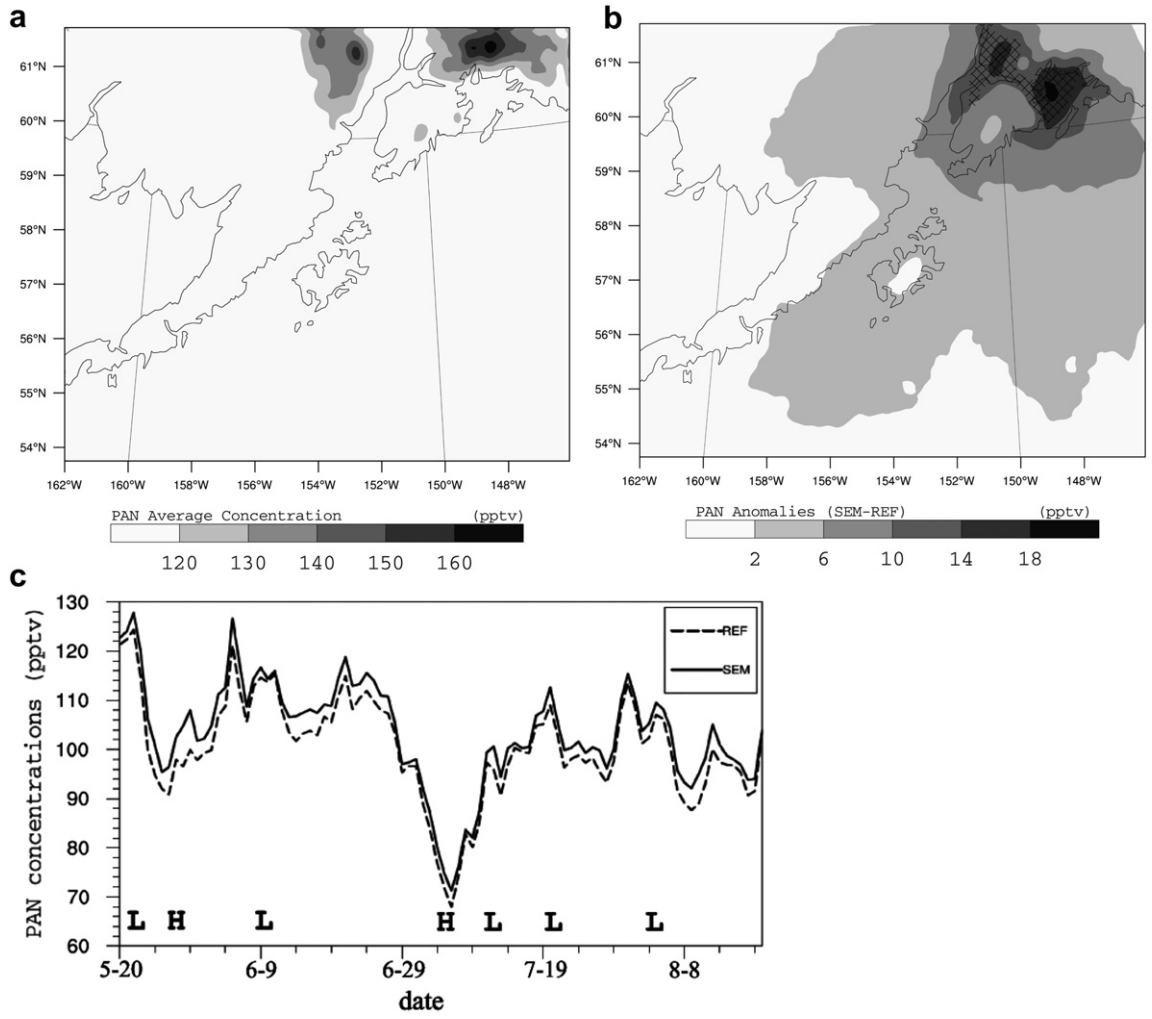

Fig. 8. PAN: Horizontal distribution of seasonal-average concentrations (a) in SEM, (b) differences SEM−REF, and (c) temporal evolution of domain-average concentrations. L and H indicate low and high-pressure. Significant changes are hashed.

They increase deposition by more than 10% elsewhere in the Gulf of Alaska with higher values along sea-lanes. As PM_{10} settles in the Anchorage, Valdez, and Prince William Sound areas, soot and ash may accumulate on glaciers affecting the beauty of the landscape, the radiation budget and snowmelt.

3.6. HNO_3, O_3, VOCs and PAN

With and without consideration of ship emissions, HNO_3 concentrations over ocean slightly exceed those over land. During high-pressure regimes, HNO_3 accumulates in the atmosphere (e.g. around July 4; Fig. 7), while during frontal passages, HNO_3 concentrations go down due to wet deposition.

Ship emissions significantly increase HNO_3 concentrations in the Gulf of Alaska and beyond (Fig. 7). In Prince William Sound, these increases exceed 100 pptv. Along the coast of the Kenai Peninsula, ship emissions increase HNO_3 about 10 pptv on average.

Ozone concentrations slightly decrease (increase) during high (low) pressure. Since over the ocean, O_3 primarily forms via reactions of the triad $NO-NO_2-O_3$, O_3 concentrations roughly depend on the ratio of NO_2 to NO. During high-pressure regimes, NO_2 is lost by HNO_3 formation and adequate amounts of NO remain in the atmosphere to destroy the ambient O_3 and diminish O_3 formation.

In Prince William Sound, O_3 concentrations increase up to 900 pptv due to ship emissions. However, given the average ambient O_3 concentrations of 15–40 ppbv available without consideration of ship emissions, this increase is marginal and insignificant. During the long daylight hours, the reactions of the triad $NO-NO_2-O_3$ very rapidly destroy O_3 after it forms. During the short nights at the beginning and end of the tourist season, NO_x reactions dominate and lead to higher HNO_3 concentrations than in the middle of the season (Fig. 7). The lack of VOC over the ocean (except from ship emissions; Fig. 11) may contribute to the low O_3 concentrations. Dry deposition of O_3 increases less than 5% due to ship emissions.

The long daylight hours permit for PAN formation. The relatively cool Alaska summer conditions lead to a long lifetime of PAN and transport into remote areas. PAN concentrations are very sensitive to temporal and spatial changes in air temperature. Increases in temperature decrease PAN due to thermal decomposition into NO_x and subsequently increase NO_x concentrations (e.g. around July 4, Figs. 6 and 8). PAN concentrations are typically higher over land because of the often-lower temperatures in the mountains than over ocean (Fig. 8).

Ship emissions result in significant increases of PAN concentrations (>18 pptv) only over Prince William Sound and the Anchorage area because HNO_3 and O_3 formation rates are much

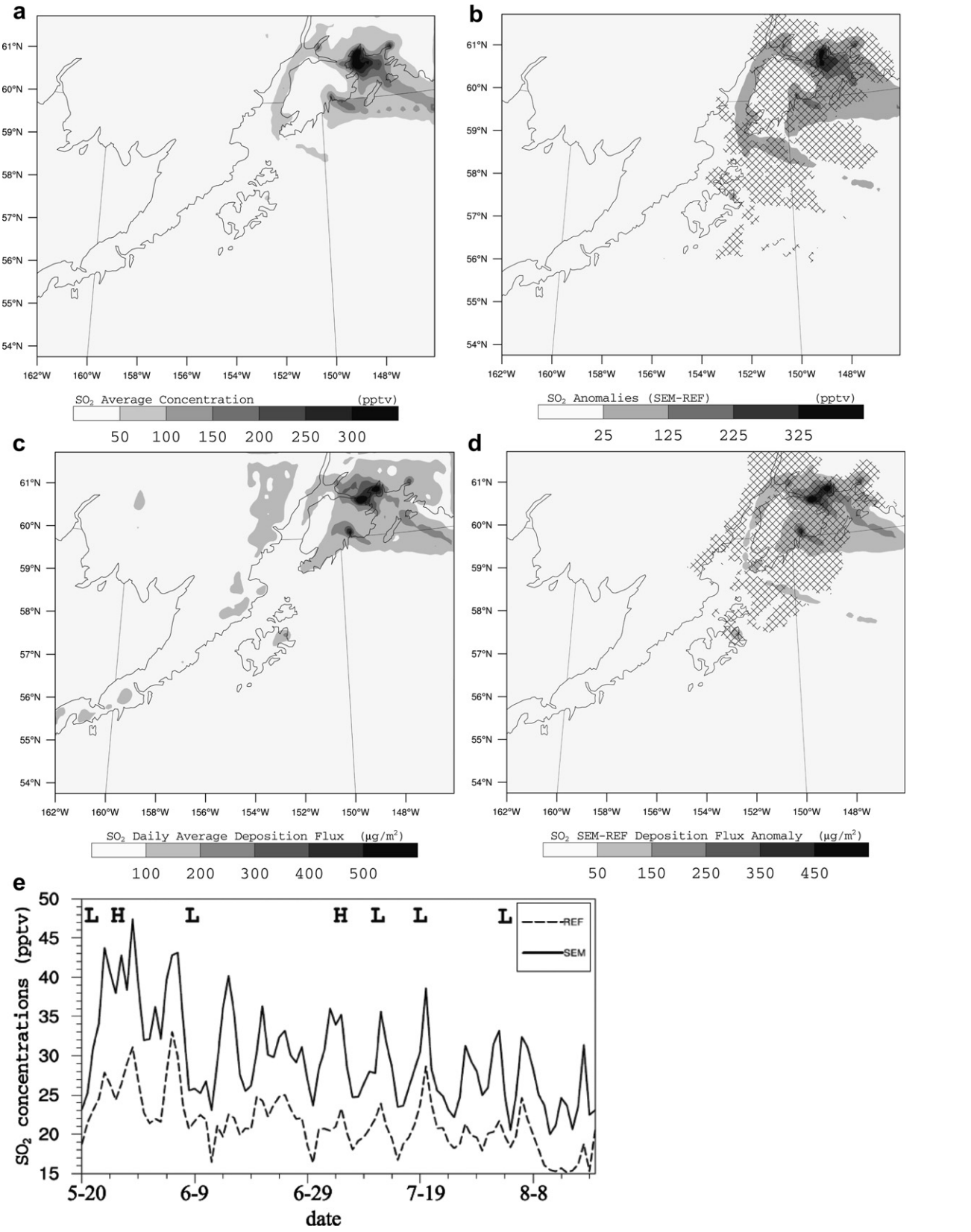

Fig. 9. SO_2: Horizontal distribution of seasonal-average concentrations (a) in SEM, (b) differences SEM−REF, (c) deposition flux, (d) deposition-flux differences, and (e) temporal evolution of domain-average concentrations. L and H indicate low and high-pressure. Significant changes are hashed.

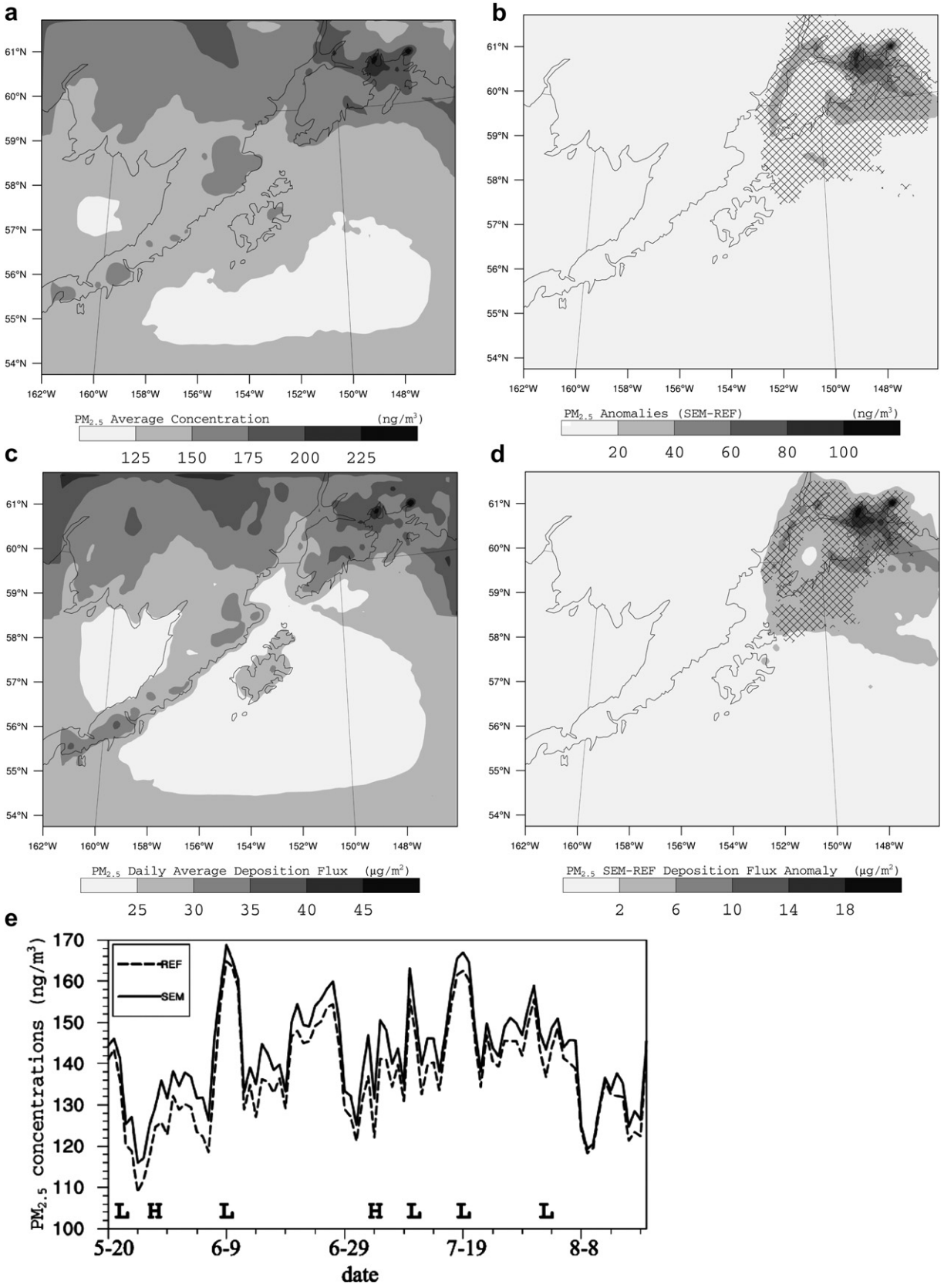

Fig. 10. $PM_{2.5}$: Horizontal distribution of seasonal-average concentrations (a) in SEM, (b) differences SEM−REF, (c) deposition flux, (d) deposition flux differences, and (e) temporal evolution of domain-average concentrations. L and H indicate low and high-pressure. Significant changes are hashed.

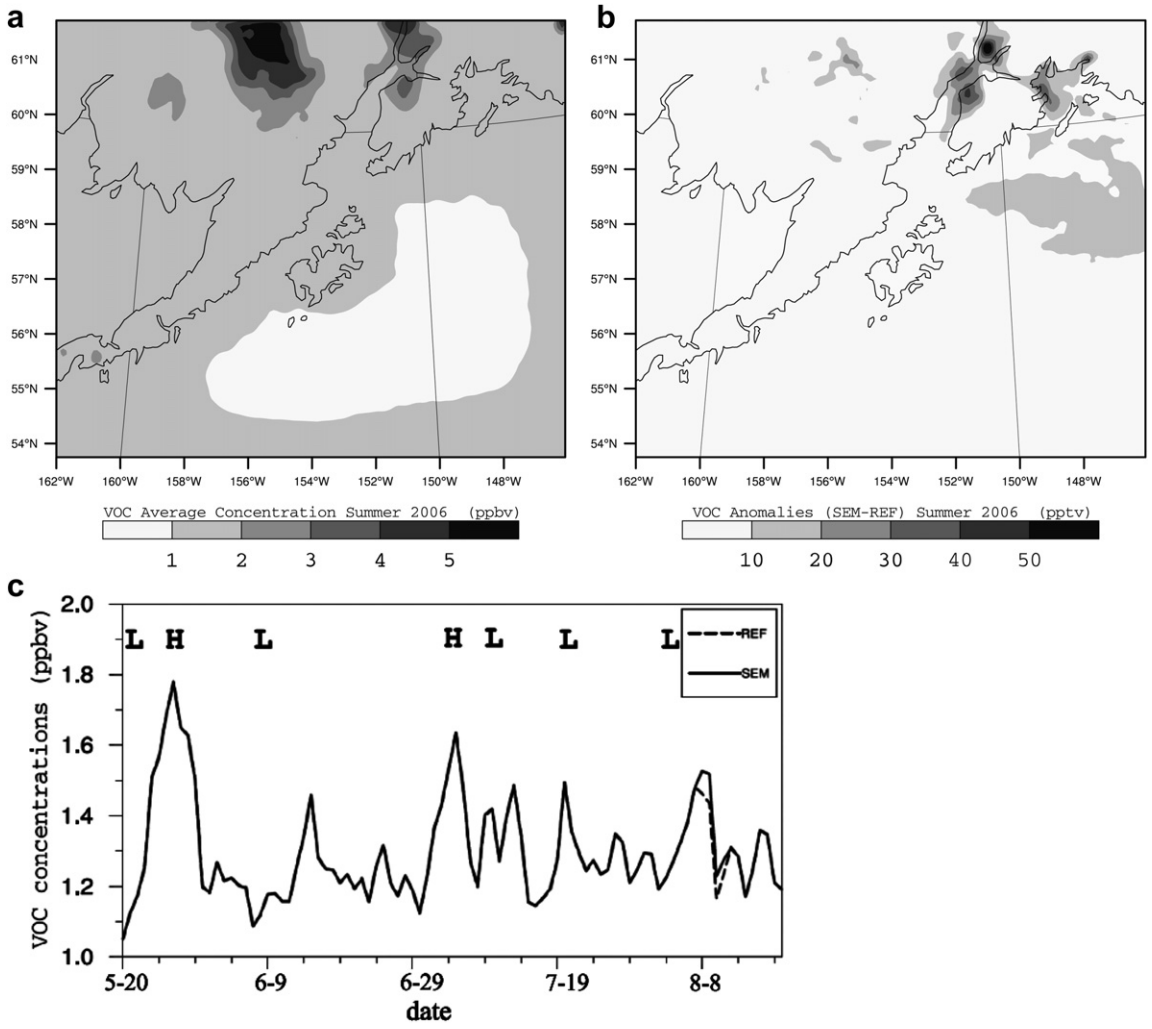

Fig. 11. VOC: Horizontal distribution of seasonal-average concentrations (a) in SEM (gray shades), (b) differences SEM−REF, and (c) temporal evolution of domain-average concentrations. L and H indicate low and high-pressure.

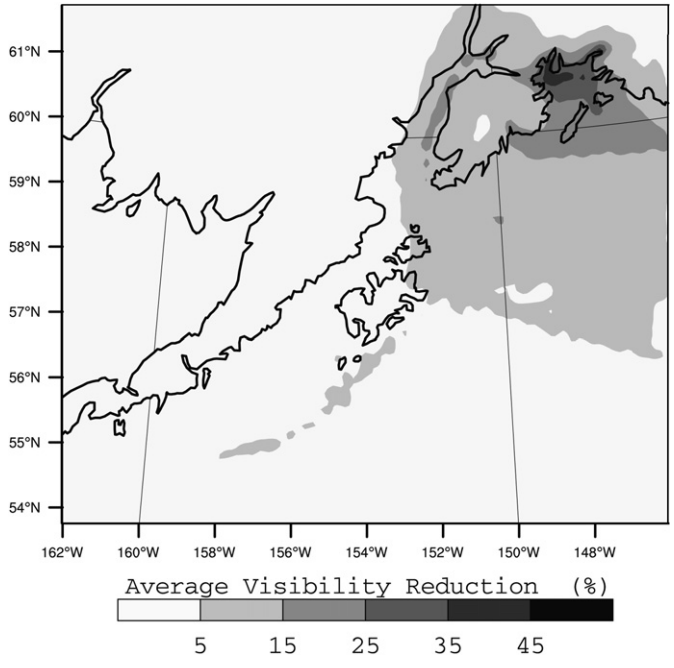

Fig. 12. Seasonal-averaged visibility reduction due to ship emissions.

higher than those of PAN. Nonetheless, during the few situations with stagnant air masses, the enhanced PAN concentrations provide NO_x long after the emitting ships left the area.

4. Conclusions

Tourism, mining, gas, and oil are essential for Alaska's economy and welfare. All economic sectors including supplies for Alaskans require ship traffic to and from Alaska. Tankers, cargo ships and, in the tourist season, cruise ships are the major anthropogenic emission sources in the Gulf of Alaska. Since current IMO regulations are very modest, ships can release appreciable amounts of pollutants into the maritime ABL. To examine the impact of ship emissions on air quality, visibility and atmospheric input into ecosystems, simulations were performed with WRF/Chem with and without consideration of ship emissions.

Evaluation by means of 24 observational sites shows that WRF/Chem captures the temporal evolution of the meteorological conditions. On average, WRF/Chem overestimates dewpoint temperature, relative humidity, pressure, wind-speed, precipitation and downward shortwave radiation, and underestimates temperature. It tends to dampen the diurnal temperature cycle. Based on our evaluation study we conclude that WRF/Chem's performance falls within the range other modern mesoscale models.

The aerosol measurements (available at only two sites and included for completeness) permitted us limited conclusions about WRF/Chem's ability to predict $PM_{2.5}$ and PM_{10} concentrations. Based on the limited data, WRF/Chem seemingly underestimates PM concentrations and has some difficulties in capturing the temporal evolution. Model technical issues, unknown emissions from wildfires, Augustine Volcano, and inaccuracies in predicted meteorology contribute to the discrepancies.

Although the simulations with ship emissions show significantly higher average concentrations and deposition fluxes than the reference simulations, trends are similar. For most of the pollutants, the synoptic situations govern their temporal and spatial distribution of concentration and deposition. SO_2 concentrations are relatively independent of the synoptic situation, but decrease throughout the season due to increasing precipitation as summer progresses. Before onset of precipitation, sea-spray increases PM concentrations during low-pressure regimes. HNO_3 accumulates during calm-wind high-pressure regimes. PAN dramatically drops during persistent warm high-pressure regimes. On average, 24 h-average $PM_{2.5}$ concentrations remain below the current NAAQS despite of ship emissions.

Ship emissions increase NO_x and SO_2 concentrations within the vicinity ($\leq$30 km) of sea-lanes (Figs. 6 and 9). Ship emissions contribute more than 90% to the NO_x deposition in Prince William Sound. Significant impacts of ship emission on PM_{10} concentrations remain localized to the port cities (Anchorage, Valdez, Whittier), but PM reduces visibility up to 30% in Prince William Sound. We conclude that ship emissions can strongly affect the attractiveness of the main tourist destinations.

Secondary pollutants (e.g. PAN, HNO_3) caused by ship emissions occur in significant amounts even far away (>30 km) from the sea-lanes (Figs. 7 and 8). The relatively cool summer temperatures typical for Alaska contribute to PAN formation. PAN becomes a huge reservoir for NO_x and enables long-range transport of nitrogen. Interestingly, ozone formation due to ship emissions remains insignificant despite long daylight hours.

Locally, some of the severity of ship-emission impacts on pollutant concentrations results from the topography in conjunction with the prevailing synoptic regimes. In Prince William Sound, for instance, low-pressure systems stagnate and eventually dissipate. The associated weak and variable winds, high surrounding mountains and heavy ship traffic lead to accumulation of pollutants. The Kenai Peninsula, for instance, commonly experiences strong, onshore winds from lows in the Gulf of Alaska. The coastal mountains lead to the ascent of air mass and eventual precipitation. Thus, emissions from ships passing around the peninsula increase deposition of contaminants on the upwind mountainside that includes Kenai Fjords National Park. The channeling of east-winds between Kenai Peninsula and Kodiak Island, for instance, enhances inland transport of primary and secondary pollutants from ship emissions toward Lake Clark and Katmai National Parks. We conclude that due to topographical features ship emissions affect some areas more than other.

As tourism and ship traffic are essential to Alaska's economy one should strive for a balance between economy and ecology. Future investigations will address proposed measures for modifying ship-emission regulations. These studies will focus on measures to improve visibility, air quality, and reduce input of atmospheric contaminants into ecosystems even if ship traffic from and to Alaska and cruise tourism increase.

Acknowledgements

We thank G. Kramm and the anonymous reviewers for fruitful discussion, and A. Reiser for editing. This research was supported by an International Polar Year student fellowship through the Cooperative Institute for Arctic Research with funds from NOAA under cooperative agreement NA17RJ1224 with the University of Alaska (UAF), the UAF Graduate School, and a grant of HPC resources from the UAF Arctic Region Supercomputing Center as part of the Department of Defense High Performance Computing Modernization Program.

Appendix

We used the Koschmieder equation (Seinfeld, 1986)

$$x = \frac{C}{\sigma_{\text{ext}}} \tag{1}$$

to calculate visibility with $C = 3.912$. The extinction coefficient (Sioutas et al., 2000)

$$\sigma_{\text{ext}} = \frac{3C_{\text{m}}Q_{\text{e}}}{2\rho_{\text{p}}d_{\text{p}}} \tag{2}$$

(m) depends on the mass concentration C_{m}(kg m^{-3}), dimensionless extinction efficiency Q_{e}, particle density ρ_{p}(kg m^{-3}), and particle diameter d_{p}(m) assumed as 4, 1550 kg m^{-3}, and 0.55×10^{-6} m, respectively.

References

Ackermann, I.J., Hass, H., Memmesheimer, M., Ebel, A., Binkowski, F.S., Shankar, U., 1998. Modal aerosol dynamics model for Europe: development and first applications. Atmospheric Environment 32, 2981–2999.

Bao, J.-W., Michelson, S.A., Persson, P.O.G., Djalaova, I.V., Wilczak, J.M., 2008. Observed and WRF-simulated low-level winds in a high-ozone episode during the Central California Ozone Study. Journal Applied Meteorology Climatology 47, 2372–2394.

Binkowski, F.S., Shankar, U., 1995. The regional particulate matter model, 1. Mode description and preliminary results. Journal Geophysical Research 100, 26191–26209.

Capaldo, K., Corbett, J.J., Kasibhatla, P., Fischbeck, P.S., Pandis, S.N., 1999. Effects of ship emissions on sulfur cycling and radiative climate forcing over the ocean. Nature 400, 743–746.

Cooper, D., Gustafsson, T., 2004. Methodology for Calculating Emissions from Ships: 1. Update of Emission Factors. Swedish Environmental Protection Agency, 35 pp.

Corbett, J.J., Köhler, H.W., 2003. Updated emissions from ocean shipping. Journal Geophysical Research 108D, 4650. doi:10.1029/2003JD003751.

Corbett, J.J., Firestone, J., Wang, C., 2007. Estimation, Validation, and Forecasts of Regional Commercial Marine Vessel Inventories, Final Report, 61 pp.

Derwent, R.G., Stevenson, D.S., Doherty, R.M., Collins, W.J., Sanderson, W.J., Johnson, C.E., Cofala, J., Mechler, R., Amann, M., Dentener, F.J., 2005. The contribution from shipping emissions to air quality and acid deposition in Europe. Ambio 34, 54–59.

Dudhia, J., 1989. Numerical study of convection observed during the winter monsoon experiment using a mesoscale two-dimensional model. Journal Atmospheric Science 46, 3077–3107.

Eder, B., Kang, D., Stein, A., McHenry, J., Grell, G., Peckham, S., 2005. The New England air quality forecasting pilot program: development of an evaluation protocol and performance benchmark. Journal Air & Waste Management Association 55, 20–27.

ENTEC UK Limited, 2002. Quantification of Emissions from Ships Associated with Ship Movements Between Ports in the European Community. European Commission, 88 pp.

Endresen, Ø., Sørgård, E., Sundet, J.K., Dalsøren, S.B., Isaksen, I.S.A., Berglen, T.F., Gravir, G., 2003. Emission from international sea transportation and environmental impact. Journal Geophysical Research 108, 4560. doi:10.1029/2002JD002898.

Eyring, V., Köhler, H.W., van Aardenne, J., Lauer, A., 2005. Emissions from international shipping: 1. The last 50 years. Journal Geophysical Research 110, D17305. doi:10.1029/2005JD005619.

Grell, G.A., Dévényi, D., 2002. A generalized approach to parameterizing convection. Geophysical Research Letters 29, 38-1–38-4.

Grell, G.A., Peckham, S.E., Schmitz, R., McKeen, S.A., Frost, G., Skamarock, W.C., Eder, B., 2005. Fully coupled "online" chemistry within the WRF model. Atmospheric Environment 39, 6957–6975.

Guenther, A., Hewitt, C., Erickson, D., Fall, R., Geron, C., Graedel, T., Harley, P., Klinger, L., Lerdau, M., McKay, W., Pierce, T., Zimmerman, P.R., 1994. A global model of natural volatile organic compound emissions. Journal Geophysical Research 100 (D5), 8873–8892.

Hines, K.M., Bromwich, D.H., 2008. Development and testing of polar weather research and forecasting (WRF) model. Part I: Greenland ice sheet meteorology. Monthly Weather Review 136, 1971–1989.
Hong, S.-Y., Lim, J.-O.J., 2006. The WRF single-moment 6-class microphysics scheme (WSM6). Journal Korean Meteorological Society 42, 129–151.
Janjić, Z.I., 2002. Nonsingular Implementation of the Mellor–Yamada Level 2.5 Scheme in the NCEP Meso Model. NCEP Office Note 437, 61 pp.
Kramm, G., Dlugi, R., Dollard, G.J., Foken, T., Mölders, N., Müller, H., Seiler, W., Sievering, H., 1995. On the dry deposition of ozone and reactive nitrogen species. Atmospheric Environment 29, 3209–3231.
Lawrence, M.G., Crutzen, P.J., 1999. Influence of NO_x emissions from ships on tropospheric photochemistry and climate. Nature 42, 167–170.
Lelieveld, J., vanArdenne, J., Fischer, H., deReus, M., Williams, J., Winkler, P., 2004. Increasing ozone over the Atlantic Ocean. Science 304, 1483–1487.
Madronich, S., 1987. Photodissociation in the atmosphere, 1, actinic flux and the effects of ground reflections and clouds. Journal Geophysical Research 92, 9740–9752.
McKeen, S.A., Chung, S.H., Wilczak, J., Grell, G., Djalalova, I., Peckham, S., Gong, W., Bouchet, V., Moffet, R., Tang, Y., Carmichael, G.R., Mathur, R., Yu, S., 2007. The evaluation of several $PM_{2.5}$ forecast models using data collected during the ICARTT/NEAQS 2004 field study. Journal Geophysical Research 112, D10S20. doi:10.1029/2006JD007608.
Mlawer, E.J., Taubman, S.J., Brown, P.D., Iacono, M.J., Clough, S.A., 1997. Radiative transfer for inhomogeneous atmospheres: RRTM, a validated correlated-k model for the longwave. Journal of Geophysical Research 102D, 16663–16682.
Mölders, N., 2008. Suitability of the weather research and forecasting (WRF) model to predict the June 2005 fire weather for Interior Alaska. Weather Forecasting 23, 953–973.
Mölders, N., Kramm, G., 2010. A case study on wintertime inversions in Interior Alaska with WRF. Atmospheric Research 95, 314–332.
Papalexiou, S., Moussiopoulos, N., 2006. Wind flow and photochemical air pollution in Thessaloniki, Greece. Part II: statistical evaluation of European zooming model's simulation results. Environmental Modeling Software 21, 1752–1758.
PaiMazumder, D., Mölders, N., 2009. Theoretical assessment of uncertainty in regional averages due to network density and design. Journal Applied Meteorology Climatology 48, 1643–1666.
Peckham, S.E., Grell, G.A., McKeen, S.A., Fast, J.D., Gustafson, W.I., Ghan, S.J., Zaveri, R., Easter, R.C., Barnard, J., Chapman, E., Wiedinmyer, C., Schmitz, R., Salzmann, M., Freitas, S.R., 2009. WRF/Chem Version 3.1 – User Guide, 81 pp.
Petzold, A., Feldpausch, P., Fritzsche, L., Minikin, A., Lauer, P., Kurok, C., Bauer, H., 2004. Particle emissions from ship engines. Journal Aerosol Science, S1095–S1096.
Porter, S.E., 2009. Investigation of the Impact of Ship Emission Atmospheric Composition and Deposition into Remote, Coastal Landscapes of Southwest Alaska. M.S. thesis. University of Alaska Fairbanks, 112 pp.
Schell, B., Ackermann, I.J., Hass, H., Binkowski, F.S., Ebel, A., 2001. Modeling the formation of secondary organic aerosol within a comprehensive air quality model system. Journal of Geophysical Research 106, 28275–28293.
Seinfeld, J.H., 1986. Atmospheric Chemistry and Physics of Air Pollution. John Wiley & Sons, 738 pp.
Shulski, M., Wendler, G., 2007. The Climate of Alaska. University of Alaska Press, 216 pp.
Simpson, D., Guenther, A., Hewitt, C.N., Steinbrecher, R., 1995. Biogenic emissions in Europe 1. Estimates and uncertainties. Journal Geophysical Research 100D, 22875–22890.
Sioutas, C., Kim, S., Chang, M., Terrell, L.L., Gong, H., 2000. Field evaluation of a modified DataRAM MIE scattering monitor for real-time $PM_{2.5}$ mass concentration measurements. Atmospheric Environment 34, 4829–4838.
Skamarock, W.C., Klemp, J.B., Dudhia, J., Gill, D.O., Barker, D.M., Duda, M.G., Huang, X.-Y., Wang, W., Powers, J.G., 2008. A Description of the Advanced Research WRF Version 3, NCAR/TN-475+STR, 125 pp.
Stockwell, W.R., Middleton, P., Chang, J.S., Tang, X., 1990. The second-generation regional acid deposition model chemical mechanism for regional air quality modeling. Journal Geophysical Research 95, 16343–16367.
Smirnova, T.G., Brown, J.M., Benjamin, S.G., Kim, D., 2000. Parameterization of cold season processes in the MAPS land-surface scheme. Journal Geophysical Research 105D, 4077–4086.
Walcek, C.J., Taylor, G.R., 1986. A theoretical method for computing vertical distributions of acidity and sulfate production within cumulus clouds. Journal Atmospheric Science 43, 339–355.
Wesley, M.L., 1989. Parameterization of surface resistances to gaseous dry deposition in regional-scale numerical models. Atmospheric Environment 23, 1293–1304.
Zhong, S., In, H., Bian, X., Charney, J., Heilman, W., Potter, B., 2005. Evaluation of real-time high resolution MM5 predictions over the Great Lakes region. Weather Forecasting 20, 63–81.